Severe Accident Symposium, Korean Nuclear Society Conference
KAERI, October 26-27, 2000

IMOD, A CONTAINMENT IODINE BEHAVIOUR MODEL
Model Description and Simulation of RTF Tests

J.C. Wren, G.A. Glowa and J.M. Ball
AECL Chalk River Laboratories, Chalk River, Ontario, Canada K0J 1J0
wrenc@aecl.ca glowag@aecl.ca ballj@aecl.ca

ABSTRACT

The time-dependent airborne concentration of iodine in the reactor containment building is one of the key parameters required to evaluate the radiological consequences of a nuclear reactor accident. A compact model that is easy to understand and use was required to incorporate iodine behaviour into containment safety analysis codes. For this reason, IMOD (Iodine Model for containment codes) was recently developed to predict the complex chemistry and mass transport behaviour of iodine in containment. IMOD uses a much smaller set of equations than is used by the fully mechanistic model LIRIC (Library of Iodine Reactions in Containment). Many individual reactions in LIRIC, representing interconversion of iodine species in the aqueous phase have been consolidated into a few simple first-order reactions in IMOD. The rate constants for these reactions have been formulated to incorporate the physics and chemistry of the LIRIC reactions such that the overall iodine kinetic behaviour is very similar. As a result, IMOD behaves like the fully mechanistic LIRIC model, but has the advantages of a small model. This paper describes the model, and presents the simulation results of two tests performed in the intermediate scale, Radioiodine Test Facility (RTF).

1. INTRODUCTION

Iodine is one of the most hazardous fission products that could be released to the outside atmosphere in the event of a nuclear reactor accident. Consequently, the time-dependent airborne concentration of iodine in the reactor containment building is one of the key parameters required to evaluate the radiological consequences of such an event. Iodine behaviour in containment under accident conditions is, however, very complex, as documented in recent critical reviews on iodine behaviour [1,2]. The behaviour of iodine in containment under accident conditions has been studied worldwide for many years. The products of these extensive studies at AECL are two models: LIRIC and IMOD.

LIRIC is a comprehensive mechanistic model [3,4]. The current version, LIRIC-3.2, has successfully simulated most of the intermediate-scale tests performed in the Radioiodine Test Facility (RTF), indicating that the model contains all of the key elements required to predict iodine behaviour [4]. Because of its complexity and size, however, it is difficult to integrate LIRIC into a safety analysis code that deals with fission-product transport in containment. This difficulty prompted the development of a new iodine module that is smaller and less complex, but maintains the predictive capabilities of the comprehensive mechanistic model. Extensive

sensitivity analysis and simulations of various intermediate scale tests performed in the RTF [1,2,5] using LIRIC, have enabled us to construct a simpler iodine model, IMOD.

The IMOD model has successfully simulated RTF tests performed over a wide range of conditions: a pH range of 4 to 10, a temperature range of 25°C to 110°C, both condensing and non-condensing conditions, surfaces ranging from non-treated or electropolished stainless steel to painted surfaces, presence of silver in the sump water, etc. This paper describes the model, and presents the simulation results of two intermediate-scale experiments performed in the RTF to demonstrate some of the model's capabilities.

2. DESCRIPTION OF IMOD

2.1 Background

The main processes determining iodine volatility in containment following an accident are:

(a) the inter-conversion between non-volatile iodine species and volatile iodine species in the aqueous phase,

Non-Volatile Iodine (aq) $\leftrightarrow$ Volatile Iodine (aq)

where non-volatile iodine species in the aqueous phase include I^-, HOI, IO_x^-, etc., and volatile iodine species in the aqueous phase include I_2 and organic iodides, and

(b) the partitioning of volatile iodine species among the gas, aqueous and adsorbed phases,

Adsorbed Iodine (aq) $\leftrightarrow$ Volatile Iodine (aq) $\leftrightarrow$ Volatile Iodine (g) $\leftrightarrow$ Adsorbed Iodine (g)

where Volatile Iodine (g) represents volatile iodine species in the gas phase, and Adsorbed Iodine (aq) and Adsorbed Iodine (g) represent the iodine species adsorbed (or absorbed) on the surfaces in contact with the aqueous and gas phases, respectively.

The relative rates of the above inter-conversion process and the partitioning of volatile iodine species among the gas, aqueous, and adsorbed phases determine the concentration of volatile iodine species in the gas phase as a function of time following an accident. As such, any iodine behaviour model must be able to simulate these processes, starting from release of iodine from a break in the fuel channel into the containment atmosphere, and ending with the release of iodine from containment to the external environment.

The inter-conversion between non-volatile and volatile iodine species in the aqueous phase (process (a)) is the main route for the production of volatile iodine species that will eventually end up in the gas phase. The formation of volatile iodine species by processes occurring in the gas phase or on surfaces is not considered to be significant under containment accident conditions [1].

Process (a) is very complex, and is affected by various factors such as pH, temperature, and the presence of organic impurities. Iodine models currently used, or being developed, for nuclear safety analysis world-wide, range from comprehensive mechanistic models such as LIRIC and INSPECT to semi-empirical models such as IODE and IMPAIR [Ref. 6 and references therein]. The strategies used by these models to describe iodine behaviour vary considerably, with the primary difference being the description of process (a). For example, the inter-conversion process is modelled using about 150 reactions in LIRIC whereas about 30 reactions are used in IODE and IMPAIR.

Although the partitioning process (process (b)) is crucial in determining iodine volatility, the partitioning processes can be adequately described and formulated using relatively simple equations once the types of volatile iodine species and their production rates are established. For this reason, the partitioning processes are formulated in very much the same way in the various iodine models, although the individual rate constants vary from model to model.

Section 2.2 presents the overall description of how the interconversion of iodine species in the aqueous phase and the partitioning and transport of volatile iodine species are modelled in the current version of IMOD, IMOD-2.0. Note that IMOD-2.0 differs from the first version of IMOD, IMOD-1.0 [7], in that it incorporates the effect of organic impurities. In the absence of organic impurities, the two versions provide identical results.

2.2 IMOD-2.0

In IMOD-2.0, iodine species are divided into 10 categories:

1) NONVOLI(aq), non-volatile iodine species in the aqueous phase,
2) VOLI(aq), volatile inorganic iodine species in the aqueous phase,
3) LVRI(aq), organic iodides less volatile than molecular iodine in the aqueous phase,
4) HVRI(aq), highly volatile organic iodides in the aqueous phase,
5) NONAQI, iodine species bound on the surfaces in contact with the aqueous phase,
6) VOLI(g), volatile inorganic iodine species in the gas phase,
7) LVRI(g), organic iodides less volatile than molecular iodine in the gas phase,
8) HVRI(g), highly volatile organic iodides in the gas phase,
9) I(con), iodine in condensing water films on surfaces, and
10) I(ad), iodine on the surfaces in contact with the gas phase.

The non-volatile iodine species in the aqueous phase, NONVOLI(aq), consists of mainly iodide ion, I^-(aq), with minor components of species such as HOI/OI^-, I_3^-, and IO_3^-. The volatile inorganic iodine species in the aqueous phase, VOLI(aq), is molecular iodine, I_2. Molecular iodine also comprises the inorganic iodine species in the gas phase, VOLI(g). Organic iodides are divided into two categories, HVRI (high volatility organic iodides) and LVRI (low volatility organic iodides), which exist both in the aqueous and gas phases. The designation LVRI includes all of the organic iodides that are less volatile than I_2, whereas HVRI refers to all of the organic iodides that are more volatile than I_2. NONAQI includes all the non-homogeneous iodine species in contact with the aqueous phase (e.g., AgI colloids/solids, if silver metal is present, or iodine adsorbed on surfaces in contact with the aqueous phase). Iodine in a condensing water film, I(con), consists of the same iodine species as NONVOLI(aq), with the distinction that these

species are in the water film on condensing surfaces, and not in the bulk aqueous phase. Iodine on dry surfaces in contact with the gas phase, I(ad), may either be physically adsorbed or weakly bonded, and able to undergo desorption, or irreversibly retained.

The IMOD model uses simple first order reactions and effective reaction rates to describe interconversion between these iodine species and their transport between phases. These iodine interconversion and transport processes are illustrated in Figure 1. Note that Figure 1 shows reactions and transport processes involving only iodine species. In addition to the processes shown, IMOD-2.0 also includes organic reactions that do not directly involve iodine. The organic reactions are modelled in IMOD-2.0 because of their indirect impact on iodine behaviour [1,2] (see discussion later in this section).

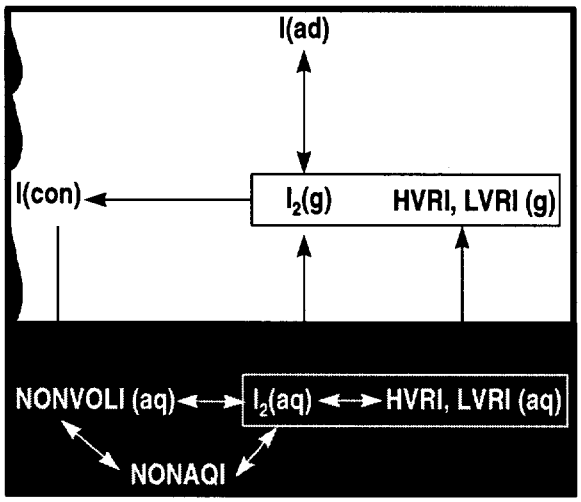

Fig 1: Iodine Interconversion and Mass Transport Processes Considered in IMOD-2.0.

The reaction and mass transport components modelled in IMOD-2.0 (and listed in Table 1), are:

1) homogeneous aqueous inorganic iodine reactions (S1),
2) dissolution of organic solvents from painted surfaces into the aqueous phase (S2),
3) radiolytic degradation of organic compounds in the aqueous phase to form organic radicals and CO_2 (S3),
4) CO_2/carbonate and acid-base equilibria (because CO_2 is the main organic radiolysis product and has a significant impact on pH) (S4),
5) reactions between iodine and organic radical to form organic iodides (S5),
6) organic iodide decomposition by hydrolysis and radiolysis (S6),
7) iodine-surface interaction in the aqueous phase (S7, S8),
8) liquid-gas interfacial mass transfer of volatile species (S9 - S11),
9) iodine sorption on dry surfaces in contact with the gas phase (S12), and
10) iodine sorption on a condensate film on a wall, and mass transport of condensate to the bulk water phase, as an additional reaction pathway for gas-phase iodine to return to the aqueous phase (S13).

Table 1: Reaction Components Modelled in IMOD-2.0

Component #	Reaction Components in IMOD-2.0	# of Reactions
	Aqueous Phase Reactions	
S1	*Aqueous Inorganic Iodine reactions:* NONVOLI(aq) ↔ VOLI(aq)	2
S2	*Organic Dissolution:* Organic Solvent on Painted Surfaces → ORG(aq)	1
S3 S4	*Organic Radiolysis:* Radiolytic Decomposition of ORG(aq) to CO_2(aq) Acid-Base Equilibria	2 5
S5 S6	*Organic Iodide Formation/Decomposition:* VOLI(aq) → HVRI(aq), LVRI(aq) HVRI(aq), LVRI(aq) → NONVOLI(aq)	2 4
	Interaction with Submerged Surfaces	
S7 S8	VOLI(aq) ↔ NONAQI NONVOLI(aq) ↔ NONAQI	2 2
	Water-Gas Partitioning	
S9	VOLI(aq) ↔ VOLI(g)	2
S10	HVRI(aq), LVRI(aq) ↔ HVRI(g),LVRI(g)	4
S11	CO_2(aq), ORG(aq) ↔ CO_2(g), ORG(g)	4
	Adsorption on Dry Surfaces	
S12	VOLI(g) ↔ I(ad)	2
	Absorption on Condensing Films	
S13	VOLI(g) → I(con) → NONVOLI(aq)	3

The rates of these reactions determine the concentrations of the chemical species involved in the reactions as a function of time. For example, for a chemical reaction:

$$A + B \rightarrow C + D$$

with a rate constant, k, the behaviour of species A, B, C and D is determined by the following rate laws:

$$-\frac{d[A]}{dt} = -\frac{d[B]}{dt} = \frac{d[C]}{dt} = \frac{d[D]}{dt} = k \cdot [A] \cdot [B]$$

where [A] is the concentration of species A at time t, and is a time dependent variable in the differential equation whereas k is typically a time-independent parameter.

Altogether, 16 individual reactions are used to model the interconversion of iodine species in IMOD-2.0, and 19 are used to model partitioning processes (Table 1). Partitioning processes in IMOD are described in the same way as in the comprehensive mechanistic model, LIRIC [4]. As

described in Section 2.1, the inter-conversion between non-volatile and volatile iodine species in the aqueous phase is the main route for the production of volatile iodine species. The success of the model, in terms of its range of applicability and the uncertainty in its prediction, strongly depends on how well this process is modelled [6].

The simple description of the aqueous interconversion process in IMOD-2.0 (S1 to S6 in Table 1) is the result of using effective rate constants to describe the combined kinetic behaviour of several individual reactions in LIRIC. The simplification was accomplished through sensitivity studies on LIRIC such that the physics and chemistry associated with the many individual reactions was retained by these effective rate constants. For example, 34 water radiolysis reactions and 79 aqueous inorganic iodine reactions in LIRIC were collapsed into two reactions describing the formation and destruction of VOLI (i.e., I_2) (S1 in Table 1). The predictive capabilities of IMOD are preserved even with this small number of reactions. Although information regarding intermediate species leading to the formation of VOLI is not calculated by IMOD, the effective reaction rate constants for production and depletion of VOLI are defined such that IMOD calculates concentrations similar to those calculated by LIRIC, over a wide range of conditions. The derivation of the smaller set of aqueous reactions and their rate constants are discussed in detail elsewhere [4,7,8].

The organic reactions in IMOD-2.0 are similar to those in LIRIC [4] where they were already implemented in simplified forms. Organic impurities in the aqueous phase can considerably change the rate of the inter-conversion between NONVOLI(aq) and VOLI(aq) because, in the presence of radiation, these impurities are readily decomposed to form organic acids and CO_2, resulting in a reduction of the pH [2,9]. The pH is the most important factor in determining iodine volatility from solution; volatility increases by approximately an order of magnitude with a one unit reduction in pH [1,2]. Furthermore, organic impurities and their radiolytic decomposition products can form organic iodides (HVRI and LVRI) [2].

Because of the potential for organic impurities to affect iodine volatility, their behaviour is described in IMOD-2.0 by the following reaction subsets:

1) organic dissolution from painted surfaces (the major source of organic impurities in the aqueous phase in an accident) (S2 in Table 1) [10],
2) the radiolytic decomposition of the organic impurities, resulting in pH changes (S3 in Table 1), and associated acid-base equilibria (S4 in Table 1) [11,12],
3) the formation and decomposition of organic iodides (S5, S6 in Table 1), and their liquid-gas interfacial mass transfer (S10 in Table 1).

It should be noted that the simplified organic sub-models included in LIRIC and IMOD-2.0 were derived from comprehensive mechanistic models. For example, the simple organic radiolysis sub-model employed by IMOD-2.0, consisting of 7 reactions (S5 and S6 in Table 1), is based on a simple MEK model [12] and a simple generic organic radiolysis model [4]. These models were developed following an extensive sensitivity analysis of an MEK (methyl ethyl ketone) model consisting of about 150 reactions [9,11].

The input parameters required by IMOD are:

a) those provided by upstream safety analysis (temperature, condensation rate, initial iodine speciation and distribution),
b) those provided by activity transport calculations within containment (dose rate, and initial iodine speciation and distribution), and
c) those dictated by containment boundary and initial conditions (gas and sump water volumes, surface types and areas, and initial pH).

For a given set of initial conditions, IMOD-2.0 calculates the total iodine concentration in each phase (i.e., in the sump, in the gas phase and on surfaces), as a function of time, from which the fraction of iodine in the gaseous form can be obtained. In addition, IMOD-2.0 has the capability of calculating the pH of the sump water and iodine speciation between I_2 and organic iodides (HVRI and LVRI) in both the sump water and the gas phase, as a function of time.

3. MODEL SIMULATION RESULTS AND DISCUSSION

Some simulation results of intermediate scale RTF experiments with an earlier version of IMOD have been previously published[1] [7,8]. In this paper, some of the capabilities of IMOD are demonstrated by the simulation of two RTF tests designated as PHEBUS RTF Test 2A and Phase 10 Test 1. PHEBUS RTF Test 2A was designed to examine the effect of pH on iodine volatility from irradiated solutions of CsI in stainless steel vessel at 90°C, whereas Phase 10 Test 1 was designed to examine the effect of painted surfaces on iodine volatility at 60°C.

The experiments were simulated by solving the kinetics of the reaction schemes listed in Table 1. This was accomplished using FACSIMILE[2], a commercially available numerical integration package for simultaneously solving coupled differential equations.

3.1 Description of the RTF Tests

The RTF facility, and typical RTF test procedures and conditions are described in detail elsewhere [1,2,5]. Briefly, the Radioiodine Test Facility is an intermediate scale facility that provides many combinations of potential reaction media (e.g., gas phase, aqueous phase and a variety of surfaces) and conditions (e.g., pH, temperature, radiation, initial concentrations, initial iodine speciation), to simulate a reactor containment building following an accident. The RTF is equipped with various on-line sensors to monitor physical and chemical properties such as temperature, pH and iodine γ-activity. Samples are also periodically taken off-line to determine the concentration of chemical species such as metal ions, hydrogen peroxide and organic iodine.

A summary of the conditions of the experiments used for this modelling exercise is presented in Table 2.

---

[1] These simulations were performed using an earlier version of IMOD, IMOD-1.0. However, because the pH was controlled during the test, and because the test was performed using a stainless steel vessel (therefore organic impurities are not present in significant quantity), the results calculated by either version of the code are identical.
[2] FACSIMILE - AEA Technologies, Harwell Laboratory, Oxfordshire, UK.

Table 2: RTF Test Conditions

	Phebus RTF2A	Phase 10 Test 1 (P10T1)
Vessel	Electropolished 316L stainless steel	Epoxy[b] painted carbon Steel
Dose rate ($kGy \cdot h^{-1}$)	~ 0.9	~ 0.6
Sump temperature	90°C	60°C
Wall temperature	110°C	60°C
Initial [CsI] ($mol \cdot dm^{-3}$)	1×10^{-5}	1×10^{-5}
Aqueous volume (dm^3)	30	25
Gas volume (dm^3)	310	315
pH	pH controlled stepwise Starting at pH 9	pH controlled at 10 for the first 45 h pH was allowed to drop after 45 h
Gas surface area[a] (dm^2)	220	220
Aqueous surface area (dm^2)	52	52
Coupons (gas)	3@250 cm^2 [c]	no coupons present
Coupons (aq)	8@19 cm^2 [c]	no coupons present

[a] vessel surface areas only (loop area excluded)
[b] Ameron Amerlock 400
[c] Hydrocentrofugon 901 Ripolin White (epoxy paint)

3.2 Simulations

3.2.1 PHEBUS RTF 2A - pH dependence

The simulation results of PHEBUS RTF 2A are shown in Figure 2. This test was performed under non-condensing conditions (i.e., sump temperature at 90°C with the wall in contact with the gas phase at 110°C) and in the absence of silver [7,8]. The pH of the water was controlled in a step-wise fashion, ranging from 4.5 to 9. The main objective of the test was to establish the pH dependence on iodine volatility at 90°C.

Note that the iodine concentrations observed after ~ 80 h into the test were affected by three 5 dm^3 additions of fresh water at 80, 90 and 95 h. This water was added to maintain the volume of the sump water. There was a leak in the aqueous recirculation loop (in the valve leading to medium waste drain) which was speculated to have started ~ 70 h into the test. The source of the leak was not identified and corrected until 95 h into the test. The leak was not simulated in the calculations.

Because the pH was being controlled during the test, the experimentally measured pH values were used during the calculation. Organic reactions were also ignored in the calculations, because the main vessel wall was electropolished stainless steel and the surface area of painted coupons submerged in the aqueous phase was very small. As a result, the dissolution of organic solvents from painted surfaces into the sump water was negligible. Under the conditions of this RTF test, the gaseous iodine was primarily comprised of molecular iodine, I_2(g) (or VOLI(g) in IMOD-2.0), whereas the aqueous iodine was comprised of mostly non-volatile iodine species such as I^- and HOI (or NONVOLI(aq) in IMOD-2.0) and, to a small extent, I_2(aq) (or VOLI(aq)).

The calculated results are in good agreement with the observed gas and aqueous phase iodine concentrations over a wide range of pH conditions at 90°C (within experimental uncertainties; a factor of two for the gas phase concentration and ±15% in the aqueous phase concentration).

3.2.2 RTF Phase 10 Test 1 - Effect of Painted Surfaces

This was an experiment performed in an epoxy-lined (Amerlock 400) carbon steel vessel at 60°C with a ^{60}Co source present. At the beginning of the test, the pH was controlled at 10 by the addition of LiOH to compensate for acid formation by the radiolysis of organic impurities. After 75 hours, the pH control was removed, and the pH was allowed to drop. The test concluded with another time period where the pH was raised and maintained at pH 10 to study desorption from the surfaces.

The simulation results are compared with the RTF data in Figures 3 through 6. The total gas phase iodine concentration is presented in Figure 3. The calculated total gas-phase iodine, which is the sum of VOLI(g), HVRI(g) and LVRI(g), is generally within the uncertainty of the experimentally obtained values. The experimental uncertainty in the total gas phase iodine concentration was generally a factor of two, based on agreement between on-line and off-line sampling.

The experimental and simulated total aqueous iodine concentration also compare very well (within the experimental uncertainties of ±15%) (Figure 4). Non-volatile iodine species such as I^- and HOI (or NONVOLI(aq)) constitute the majority of the aqueous iodine species, with the volatile iodine species such as molecular iodine and organic iodides (VOLI(aq), HVRI(aq), LVRI(aq)) contributing only a small fraction to the aqueous iodine concentration. This also made it difficult to perform any quantitative speciation measurements for aqueous iodine species.

The observed concentration of organic iodides and I_2 in the gas phase data is shown in Figure 5, along with the values calculated by the model. Agreement between the observed and simulated species concentrations is reasonable, despite the high uncertainty in the gas phase speciation data.

Finally, the observed and calculated values for the aqueous pH are shown in Figure 6. The good agreement between the modelled and experimental results indicates that the radiolytic decomposition of organic compounds to CO_2 is also modelled adequately in IMOD.

(a)

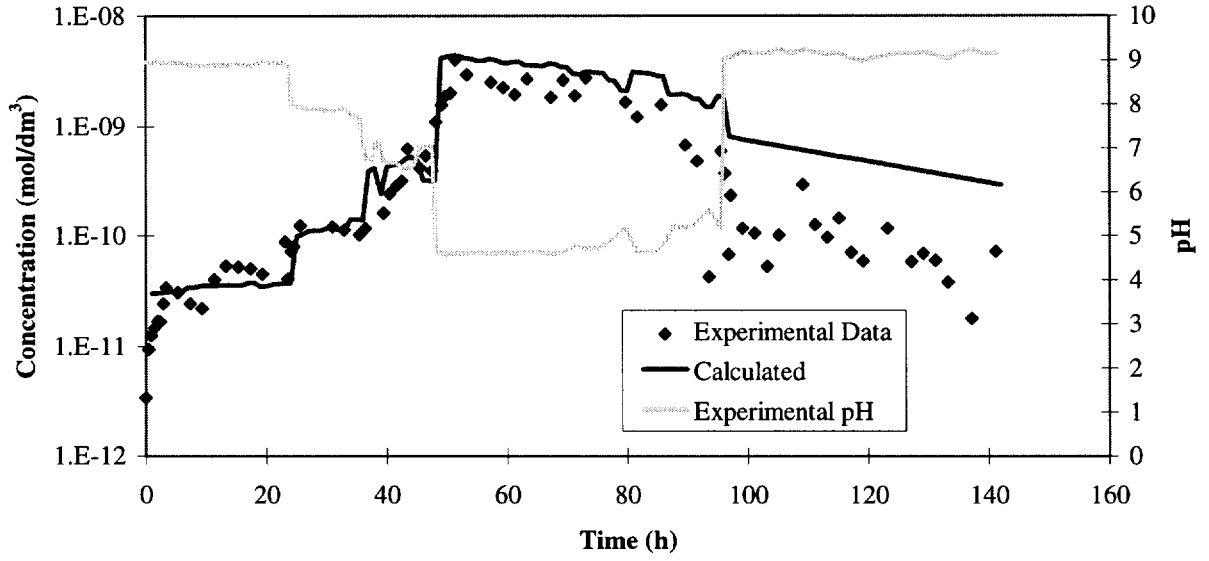

(b)

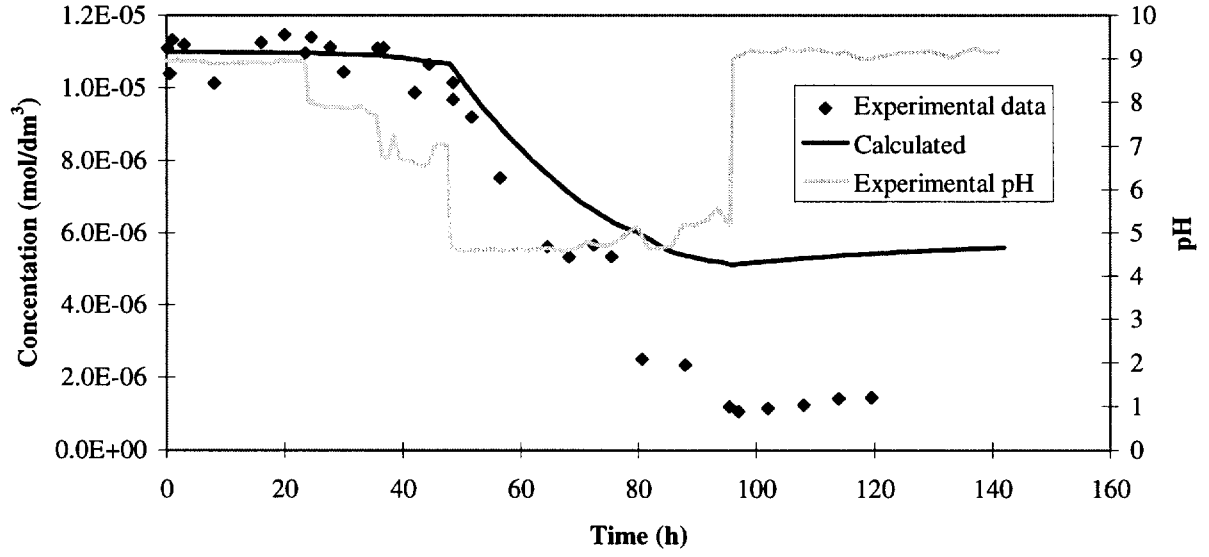

Fig. 2: Iodine Concentrations (a) in the Gas and (b) in the Aqueous Phase (PHEBUS RTF Test 2A). Note that the sudden drop in the iodine concentration at ~ 80 h was mainly due to the addition of fresh water, which was not modelled.

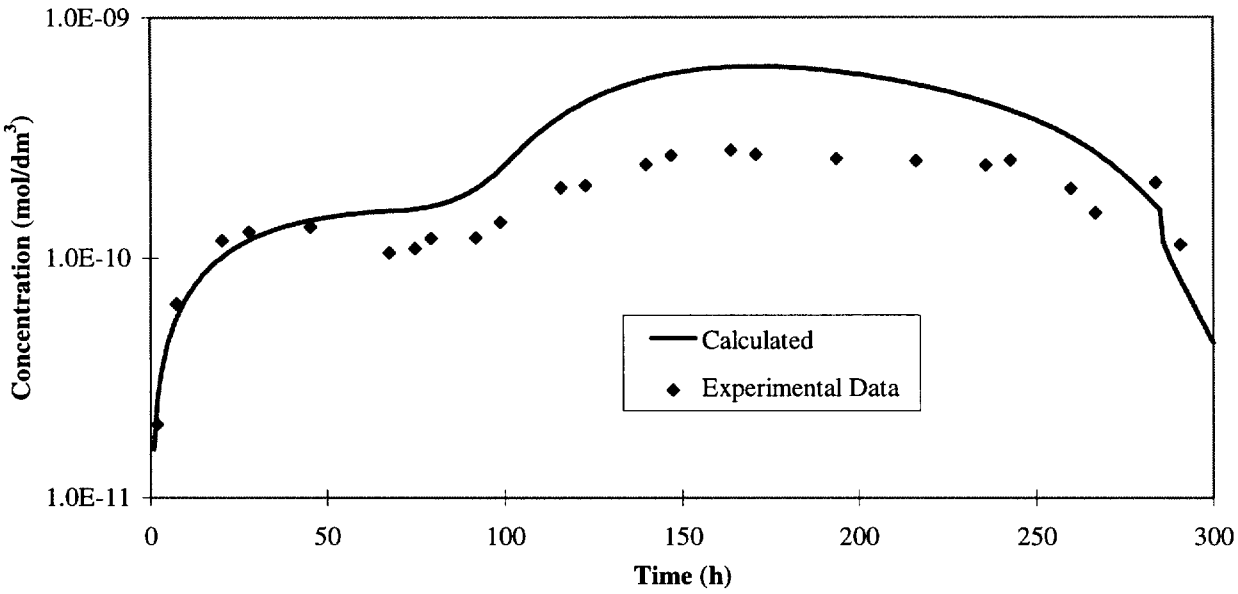

Fig 3: Calculated and Observed Total Gas Phase Iodine Concentrations for Phase 10 Test 1, an Irradiated (0.6 $kGy \cdot h^{-1}$) Solution Containing CsI (10^{-5} $mol \cdot dm^{-3}$) in an Epoxy Lined (Amerlock 400 by Ameron), Carbon Steel Vessel at 60°C.

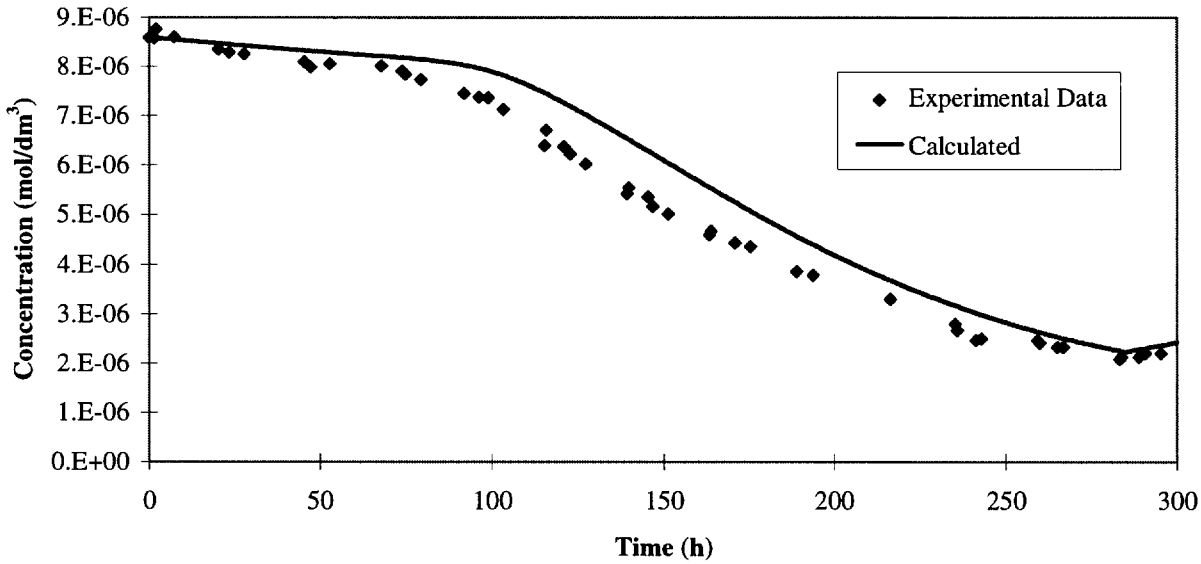

Fig 4: Calculated and Observed Total Aqueous Phase Iodine Concentrations for Phase 10 Test 1, an Irradiated (0.6 $kGy \cdot h^{-1}$) Solution Containing CsI (10^{-5} $mol \cdot dm^{-3}$) in an Epoxy Lined (Amerlock 400 by Ameron), Carbon Steel Vessel at 60°C.

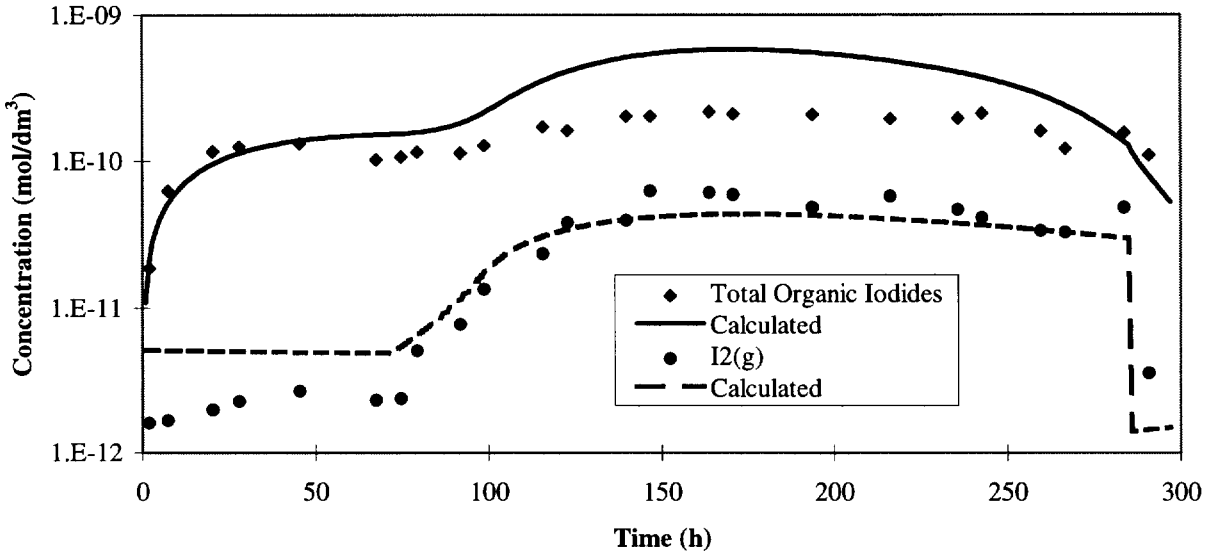

Fig 5: Calculated and Observed Gas Phase Iodine Species for Phase 10 Test 1, an Irradiated (0.6 $kGy \cdot h^{-1}$) Solution Containing CsI (10^{-5} $mol \cdot dm^{-3}$) in an Epoxy Lined (Amerlock 400 by Ameron), Carbon Steel Vessel at 60°C.

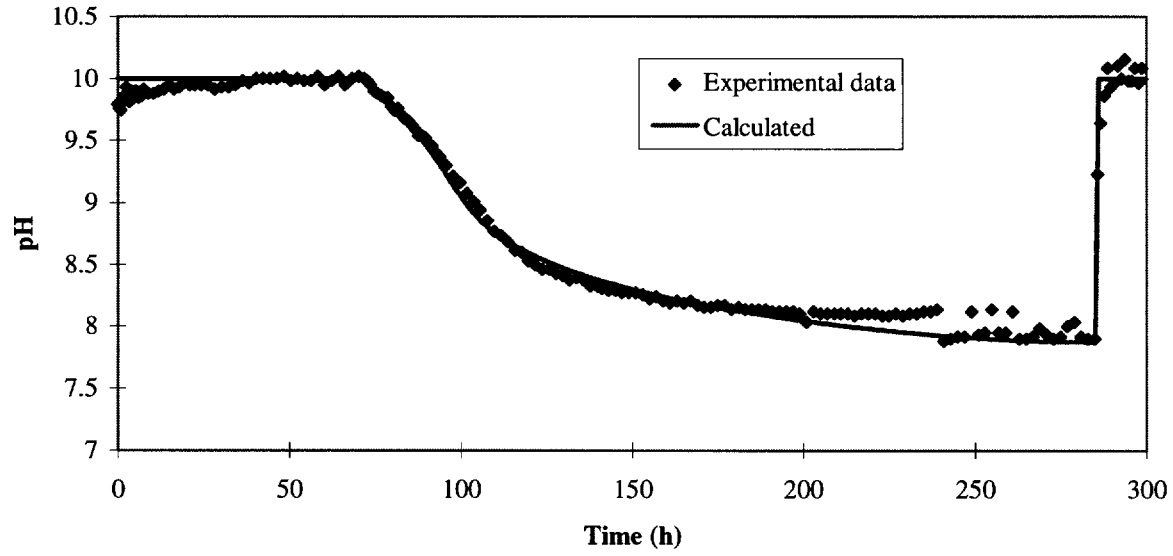

Fig 6: Calculated and Observed Aqueous pH for Phase 10 Test 1, an Irradiated (0.6 $kGy \cdot h^{-1}$) Solution Containing CsI (10^{-5} $mol \cdot dm^{-3}$) in an Epoxy Lined (Amerlock 400 by Ameron), Carbon Steel Vessel at 60°C.

4. SUMMARY AND CONCLUSIONS

The simplified model for containment iodine chemistry and transport, IMOD, has been described and the model simulation results of two RTF tests have been presented.

The current version of the model, IMOD-2.0, is comprised of equations representing 16 chemical reactions and 19 partitioning processes. This simple model for the simulations of the complex iodine behaviour in containment was developed based on extensive sensitivity analysis of a comprehensive mechanistic model, LIRIC. Each iodine reaction path in IMOD represents many reaction steps in LIRIC, with the physics and chemistry of these reactions incorporated into the rate constants. That is, the rate constants for the reactions in IMOD are effective rate constants, defined as a function of radiation dose, temperature, pH, type of surface, surface area, gas and aqueous volume, which are based on parametric studies of LIRIC.

Some of the capabilities of IMOD-2.0 were demonstrated by the simulation of PHEBUS RTF Test 2A (electropolished stainless steel vessel at 90°C, pH controlled stepwise) and RTF Phase 10 Test 1 (epoxy-painted carbon-steel vessel at 60°C). The simulation results are in reasonable agreement with the observed total gas and aqueous phase iodine concentrations and organic iodide concentrations. Considering the simplicity of the model and the complexity of the processes, the model is considered to be performing very well.

ACKNOWLEDGEMENTS

The authors would like to thank Tracy Sanderson for reviewing this document and for her helpful discussions.

REFERENCES

1. J.C. Wren, J.M. Ball, and G.A. Glowa, "The Chemistry of Iodine in Containment", Nucl. Tech., 129, 297 (2000).
2. J.C. Wren, J.M. Ball, and G.A. Glowa, "The Interaction of Iodine with Organic Material in Containment", Nucl. Tech., 125, 337 (1999).
3. J.C. Wren, G.A. Glowa, and J.M. Ball, "Modelling Iodine Behaviour Using LIRIC 3.0", in Proceedings of the Fourth CSNI/OECD Workshop on the Chemistry of Iodine in Reactor Safety, Wurenlingen, Switzerland, (1996).
4. J.C. Wren and J.M. Ball, "LIRIC, the Iodine Chemistry and Mass Transport Model in Containment under Reactor Accident Conditions", Accepted for Publication, Rad. Phys. Chem. (2000).
5. J.M. Ball, W.C. H. Kupferschmidt and J.C. Wren "Results From Phase 2 of the Radioiodine Test Facility Experimental Program", in Proceedings of the Fourth CSNI/OECD Workshop on the Chemistry of Iodine in Reactor Safety, Wurenlingen, Switzerland, (1996).
6. J.M. Ball, et al., "International Standard Problem (ISP) No. 41: Computer Code Comparison Exercise Based on a Radioiodine Test Facility (RTF) Experiment on Iodine Behaviour in Containment under Severe Accident Conditions", in Proceedings of OECD Workshop on Iodine Aspects of Severe Accident Management, Vantaa, Finland, May 18-20, 1999, NEA/CSNI/R(99)7, pp. 311 - 325, CSNI/OECD Report (1999).
7. J.C. Wren, G. Glowa and J.M. Ball, "A Simplified Iodine Chemistry and Transportation Model: Model Description and Some Validation Calculations", in Proceedings of OECD Workshop on Iodine Aspects of Severe Accident Management Vantaa, Finland, May 18-20, 1999, NEA/CSNI/R(99)7, pp. 327 - 341, CSNI/OECD Report (1999).
8. J.C. Wren, G.A. Glowa and J.M. Ball, "Summary of PHEBUS RTF Programme", in Proceedings of the 4th PHEBUS Seminar, Marseille, France, March 20-21, 2000.
9. P.A. Driver, G.A. Glowa and J.C. Wren, "Steady-State γ-Radiolysis of Aqueous Methyl Ethyl Ketone (2-Butanone) Under Postulated Nuclear Reactor Accident Conditions", Rad. Phys. Chem., 57, 37 (2000).
10. J.C. Wren, D.J. Jobe, G.G. Sanipelli and J.M. Ball, "Dissolution of Organic Solvents from Painted Surfaces into Water", Can. J. Chem. 78, 464 (2000).
11. G.A. Glowa, P.A. Driver, and J.C. Wren, "Irradiation of MEK Part II: A Detailed Kinetic Model for the Degradation of 2-Butanone in Aerated Aqueous Solutions under Steady-State γ-Radiolysis Conditions", Rad. Phys. Chem., 58, 49 (2000).
12. J.C. Wren and G.A. Glowa "A Simplified Kinetic Model for the Degradation of 2-Butanone in Aerated Aqueous Solutions under Steady-State γ-Radiolysis Conditions", Rad. Phys. Chem. 58, 341 (2000).